

Intrinsic color diversity of nearby type Ia supernovae

Noriaki ARIMA,^{1,2*} Mamoru DOI,^{1,3,4} Tomoki MOROKUMA,¹ and Naohiro TAKANASHI⁵

¹Institute of Astronomy, Graduate School of Science, The University of Tokyo, 2-21-1 Osawa, Mitaka, Tokyo 181-0015, Japan

²Department of Astronomy, Graduate School of Science, The University of Tokyo, 7-3-1 Hongo, Bunkyo-ku, Tokyo 113-0033, Japan

³Research Center for the Early Universe, Graduate School of Science, The University of Tokyo, 7-3-1 Hongo, Bunkyo-ku, Tokyo 113-0033, Japan

⁴Kavli Institute for the Physics and Mathematics of the Universe, The University of Tokyo, 5-1-5 Kashiwanoha, Kashiwa, Chiba 277-8583, Japan

⁵Executive Management Program, The University of Tokyo, 7-3-1 Hongo, Bunkyo-ku, Tokyo 113-8654, Japan

*E-mail: n_arima@ioa.s.u-tokyo.ac.jp

Received (reception date); Accepted (acceptation date)

Abstract

It has been reported that the extinction law for Type Ia Supernovae (SNe Ia) may be different from the one in the Milky Way, but the intrinsic color of SNe Ia and the dust extinction are observationally mixed. In this study, we examine photometric properties of SNe Ia in the nearby universe ($z \lesssim 0.04$) to investigate the SN Ia intrinsic color and the dust extinction. We focus on the Branch spectroscopic classification of 34 SNe Ia and morphological types of host galaxies. We carefully study their distribution of peak colors on the $B - V$, $V - R$ color-color diagram, as well as the color excess and absolute magnitude deviation from the stretch-color relation of the bluest SNe Ia. We find that SNe Ia which show the reddest color occur in early-type spirals and the trend holds when divided into Branch sub-types. The dust extinction becomes close to the Milky-Way like extinction if we exclude some peculiar red Broad Line

(BL) sub-type SNe Ia. Furthermore, two of these red BLs occur in elliptical galaxies, less-dusty environment, suggesting intrinsic color diversity in BL sub-type SNe Ia.

Key words: supernovae: general — galaxies: general — dust, extinction

1 Introduction

Type Ia supernovae (SNe Ia) have been used as distance indicators thanks to their high luminosity, which can be observed at cosmological distances ($M_B \approx -19.3$ mag). Luminosity can be standardized after correcting the empirical relation between luminosity and light-curve decline rate: a brighter SN Ia diminishes slowly (so-called Phillips-relation: Phillips 1993; Hamuy et al. 1996; Riess et al. 1996; Phillips et al. 1999). Their use for cosmological studies provided us an observational evidence that the expansion speed of the Universe is accelerating (Riess et al. 1998; Perlmutter et al. 1999).

Near the epoch of maximum brightness, SNe Ia show strong silicon absorption lines, especially the Si II $\lambda 6355$ but neither hydrogen nor helium lines are present (Filippenko 1997; Gal-Yam 2017). SNe Ia are thought to originate from carbon-oxygen (C/O) white dwarfs in close binary systems. Theoretically, two most popular SN Ia scenarios are the single-degenerate (SD) model and the double-degenerate (DD) model. In the SD model, a white dwarf accretes material from a non-degenerate companion star until it reaches near the Chandrasekhar limiting mass ($M_{\text{Ch}} \approx 1.4M_{\odot}$) and explodes (Whelan & I. Iben 1973; Nomoto 1982). In the DD model, two white dwarfs merge after losing orbital energy and angular momentum by gravitational waves (I. Iben & Tutukov 1984; Webbink 1984). However, we still don't have clear physical understandings of the evolutionary paths to SNe Ia and there are several other potential progenitor models (see reviews of Maoz & Mannucci 2012; Maeda & Terada 2016 and also Livio & Mazzali 2018). In addition, the Phillips-relation lacks complete physical understanding.

Identifying the differences and diversity of SNe Ia is important for understanding their progenitor scenarios and improving their effectiveness as a cosmological tool. Recent cosmological measurements with SNe Ia are not only limited by the sample size, but also by the systematic uncertainties due to the lack of our understanding the variety and physical mechanisms of SNe Ia (Conley et al. 2010; Betoule et al. 2014). Although observables that characterize each SN Ia such as color may give us a clue, scatters in colors and dust properties surrounding SNe Ia prevent us to reduce uncertainties for precision cosmology (e.g., see figure 1 of Sullivan et al. 2011).

It is also critical for SN Ia studies to understand the properties of interstellar and circumstellar

dust. In general, extinction by dust is described by a parameter R_V : total-to-selective extinction ratio defined by $R_V = A_V/E(B - V)$, which reflects the property of dust. Large value of R_V means large grain size of dust (c.f., Clayton et al. 2003). The mean value in our Milky Way is $R_V = 3.1$ (Cardelli et al. 1989). It has been reported by previous studies that the dust extinction for SNe Ia has smaller value of R_V than the mean value of Milky Way. For example, Nobili & Goobar (2008) and Kessler et al. (2009) reported $R_V = 1.75$ and $R_V = 2.2$, respectively (see also table 1 of Cikota et al. (2016) for the summary of small R_V reported until then). Assuming a constant R_V , Folatelli et al. (2010) analyzed the optical–NIR colors of the nearby Carnegie Supernova Project (CSP: Contreras et al. 2010) SN Ia sample and they obtained $R_V \approx 1.7$, but they obtained $R_V = 3.2 \pm 0.4$ when the extremely red objects ($E(B - V) \gtrsim 1$) were excluded. Mandel et al. (2011) later did a more sophisticated analysis and showed variations in R_V , with the low-extinction events giving higher values of $R_V \sim 3$ and high-extinction events giving $R_V \sim 2$. Burns et al. (2014) found a similar result. In recent studies, Stanishev et al. (2018) used optical-NIR light curves to derive $R_V \simeq 1.8 - 1.9$ and Cikota et al. (2016) also favors small R_V but they obtained different R_V values for SNe Ia with different host morphology ($R_V = 2.71 \pm 1.58$ for SNe Ia observed in Sab–Sbp galaxies, and $R_V = 1.70 \pm 0.38$ for SNe Ia observed in Sbc–Scp galaxies). On the other hand, based on a spectral series, Sasdelli et al. (2016) showed R_V to be consistent with the typical Milky Way value. Mandel et al. (2017) constructed host galaxy dust models for SNe Ia and the dust extinction they obtained ($R_B = 3.8 \pm 0.3$; $R_B = R_V + 1$) also agrees with the Milky Way dust extinction.

Over the years, observations provided that there are varieties in luminosity and spectral features of SNe Ia. For example, 1991T-like and 1991bg-like SNe are well-known prominent outliers. The 1991T-like SNe are more luminous ($\gtrsim 0.6$ mag.) than normal SNe Ia and show lines of doubly ionized elements (especially Fe III) in their spectra at early times (Filippenko et al. 1992; Phillips et al. 1992). As opposed to it, the 1991bg-like SNe are less-luminous and show rapidly evolving light-curve and strong Ti II lines (Nugent et al. 1995; Mazzali et al. 1997). Diagnosing spectra around maximum brightness has been used to investigate the origins of the diversity.

In Branch et al. (2006), SNe Ia were assigned into four groups according to measurements of the equivalent width (EW) of two Si II absorption features at about 5750 Å and 6100 Å which are attributed to rest-frame $\lambda 5972$ and $\lambda 6355$ lines, respectively. The four groups are: core-normal (CN), broad-line (BL), cool (CL), and shallow-silicon (SS). The 1991T-like and the 1991bg-like SNe Ia are assigned into the extreme end of SS and CL, respectively. Using early phase SN Ia colors, Stritzinger et al. (2018) found that there are two distinct populations with different early color evolution in $B - V$, and the two early blue/red events are correlated with the Branch spectroscopic groups.

Another spectroscopic approach is dividing SNe Ia into two groups in terms of the expansion

velocity estimated from the absorption minimum of Si II $\lambda 6355$ line. Wang et al. (2009) found that high velocity (HV) SNe Ia show redder $B - V$ colors at maximum brightness than normal velocity (NV) SNe Ia. Zheng et al. (2018) found that SNe Ia with higher velocities are inferred to be intrinsically fainter than the NV SNe Ia and they confirm that HV SNe Ia are probably intrinsically different from NV SNe Ia.

Focusing on the differences in environment is another approach to study the diversity of SNe Ia. It is found that host galaxy stellar mass correlates with SNe Ia luminosity: SNe Ia in massive host galaxies are intrinsically more luminous after light-curve/color corrections (Kelly et al. 2010; Sullivan et al. 2010; Childress et al. 2013; Pan et al. 2014; Betoule et al. 2014). The latest cosmological study by Smith et al. (2020) found that SNe Ia in high-mass galaxies ($> 10^{10} M_{\odot}$) are intrinsically more luminous than their low-mass counterparts by 0.040 ± 0.019 mag. Correlations with host-galaxy metallicity have also been studied (e.g., Moreno-Raya et al. 2016). Theoretically, the metallicity of the SN Ia progenitors affects the strength of spectral features more in the UV wavelengths than in the optical (Lentz et al. 2000; Walker et al. 2012; Miles et al. 2016). However, each model has a different effect on the strength and wavelength range. A recent study using SNe Ia with normal light-curve shapes found that there is no significant correlations between the UV-optical colors of SNe Ia and the host-galaxy metallicity (Brown & Crumpler 2020), which is in contrast to the findings of Pan et al. (2020). The physical relation between host metallicity and SN Ia properties is not yet clear.

For fitting a light-curve shape to standardize SN Ia luminosity, "MLCS2k2" (Jha et al. 2007), "SALT2" (Guy et al. 2007) and "SNooPy" (Burns et al. 2011; Burns et al. 2014) are methods often used. Each method parameterizes observed light curves and estimates host-galaxy dust extinction at the same time. When we investigate the host-galaxy dust extinction, we should treat dust extinction effect and SN Ia intrinsic colors independently, and hence we should not assume any dust extinction models. In contrast, Takanashi et al. (2017) (hereafter TAK17) simply parameterizes only light curve shapes and peak brightness. They analyzed multi-band light curves of SNe Ia from SDSS-II SN Survey and their result suggests that there seems to be inherently different sub-types among SNe Ia with different colors and extinction laws of host galaxy dust, which is consistent with previously suggested ideas (e.g., Mannucci 2005; Quimby et al. 2007).

As we mentioned above, the diversity of SN Ia spectra, luminosity and colors may be correlated with host properties and also different types of dust extinction. In order to improve accuracy as distance indicators for cosmological studies, understanding the diversity is very important. In TAK17, they only studied photometric properties. In this paper we extend the study of TAK17 combining with the spectroscopic classification of SNe Ia defined by Branch et al. (2009). In Section 2, we describe our SNe Ia sample with host galaxy morphology used in this study. In Section 3, we apply the method

used in TAK17 to analyze photometric SNe Ia data and show the results of nearby SNe Ia with spectral classification and host morphology. In Section 4, we discuss our results and we summarize our findings in Section 5.

2 Data

2.1 Photometric data

We use the photometric data obtained from Takanashi et al. 2008 (hereafter, TAK08). In TAK08, they collected U –, B –, V –, R – and I -band photometry of 122 nearby ($z < 0.11$) SNe Ia from published sources. Magnitudes are presented in the Vega system, and are all K –corrected. As we mentioned in Section 1, well-known light curve fitting methods fit observed SNe Ia light curves by parameterizing their light-curve shape, peak brightness, color and extinction at the same time. In TAK08 (and also in TAK17), unlike these methods, their original "Multi-band Stretch Method" simply characterizes light-curve shapes and peak brightness corrected for Galactic dust extinction from Schlegel et al. (1998) without dust extinction correction in the host galaxies. This makes it possible to investigate the diversity of SN Ia light curves directly.

We use B –, V – and R –band absolute magnitude and B –band stretch factor (Goldhaber et al. 2001), which is a parameter describing a width of SN Ia light-curve shape. In TAK08, they adopt the values of cosmological parameters, $H_0 = 70.8 \text{ km s}^{-1} \text{ Mpc}^{-1}$, $\Omega_M = 0.262$, $\Omega_\Lambda = 0.738$ from Spergel et al. (2007) for calculating absolute magnitude. We adopt these values in this paper.

2.2 Spectroscopic data

As described in section 1, Branch et al. (2006) divide SNe Ia into four groups based on equivalent widths (=EWs) of the two Si II $\lambda 6355, \lambda 5972$ lines (=EW(6100) and EW(5750)); Core Normal (CN), Broad Line (BL), Cool (CL) and Shallow Silicon (SS). In this paper, we use the term "sub-type" to refer to each Branch spectroscopic group. CN SNe Ia have typical EWs for both Si II lines. BL SNe Ia have 6100 Å absorption that is broader and deeper than CN SNe Ia and that means they have large EW(6100). For CL SNe Ia, the name "Cool" comes from their low temperature compared with other sub-types and they show relatively large EWs for both lines. On the other hand, SS SNe Ia have shallow Si II absorption lines, which implies the ejecta is in high temperature. In Branch et al. (2009), they say that there is no distinct threshold of these two equivalent widths that classifies them into four sub-types.

In this study, combining photometry from TAK08 with the Branch spectroscopic sub-types (Branch et al. 2009), we collect nearby ($0.0021 < z < 0.031$) 34 SNe Ia (hereafter, referred to as

"Branch sample"). The Branch sample consists of 9 CN, 10 BL, 3 CL and 12 SS SNe Ia. Although there are slightly different spectroscopic classifications among Branch et al. (2009) and the other papers, we adopt the classification presented in Branch et al. (2009) to keep consistency. In Branch et al. (2009), most of the spectra taken ± 3 days from maximum phase are used¹, while for example, in Blondin et al. (2012), spectra taken within ± 5 days from maximum phase are used. The properties of our sample are summarized in table 1.

2.3 ΔM_B and $SNCE$

In TAK17, they analyzed multi-band light curves of 328 SNe Ia observed by the Sloan Digital Sky Survey-II Supernova Survey (Sako et al. 2008; Sako et al. 2018). Equations (1) and (2) show the relations between the inverse B -band stretch factor $s_{(B)}^{-1}$ and B -, V -band absolute magnitude of the SDSS bluest SNe Ia, which they call stretch-magnitude relations. The color range of the bluest SNe Ia is $-0.14 \leq (M_B - M_V) \leq -0.10$. They introduced two parameters: ΔM_B and $SNCE$ (= SuperNova Color Excess). They define ΔM_B as the magnitude difference between B -band absolute magnitude, M_B and estimated absolute magnitude with the stretch-magnitude relation of the bluest SN Ia sample. Also, $SNCE$ is defined by the difference between observed $B - V$ color and intrinsic color from the stretch-color relation. The idea is based on an assumption that relations among a light-curve shape parameter, color and luminosity obey a unique relation for all SNe Ia. The relation can be derived from the bluest SNe Ia, for which extinction may be negligible. In case of the bluest SNe Ia, by definition, both ΔM_B and $SNCE$ become close to zero. Non-zero ΔM_B and $SNCE$ can be interpreted as either dust extinction or intrinsically different luminosity and color from the bluest SNe Ia.

$$M_{B(\text{bluest SNe Ia})} = (1.71 \pm 0.31) \times s_{(B)}^{-1} - (20.73 \pm 0.31) \quad (1)$$

$$M_{V(\text{bluest SNe Ia})} = (1.59 \pm 0.26) \times s_{(B)}^{-1} - (20.51 \pm 0.25) \quad (2)$$

Using the equations (1) and (2), the ΔM_B and the $SNCE$ are derived as equations (3) and (4)

$$\Delta M_B = m_B - \mu - (1.71 \times s_{(B)}^{-1} - 20.73) \quad (3)$$

$$SNCE = (m_B - m_V) - (0.12 \times s_{(B)}^{-1} - 0.22) \quad (4)$$

, where m_B and m_V are stretch-corrected apparent B -band and V -band magnitudes at B -band maximum and μ is distance modulus. We derive the ΔM_B and $SNCE$ using the relations. The list of ΔM_B and $SNCE$ of the Branch sample is shown in table 2.

¹ Some of the Branch samples (SN 1997br, 1997do, 1998ab, 1999gh, 2000cn and 2001V) have no Si II EWs measurements within ± 3 days from maximum phase.

2.4 Host galaxy morphology

Because there are strong correlations between SNe Ia and their host galaxy properties (e.g., Sullivan et al. 2006), the inclusion of host galaxy morphology will give us implications to study the SN Ia intrinsic color diversity. We obtained the Hubble type of host galaxies from the NED (NASA/IPAC Extragalactic Database) and then use their host type index T (de Vaucouleurs 1959) to divide SNe Ia into different host morphological groups. We divide SNe Ia into three groups: early-type galaxies (E/S0; $T \leq 0$), early-type spirals (from Sa to Sb; $1 \leq T \leq 4$) and late-type spirals or irregular galaxies (Sc or later and Irr; $T \geq 5$).

3 Results

3.1 Color-color diagram

In figure 1, we show a $B - V$ vs $V - R$ color-color diagram. Two different extinction laws with $R_V = 3.1$ and $R_V = 2.0$ are shown by black solid and red dashed lines respectively. Extinction law with larger R_V has steeper slope in this diagram. In figure 1, the distribution seems to be more consistent with the extinction law with $R_V = 2.0$ than $R_V = 3.1$ for our sample. There are, however, apparently three BL objects (SN 1999cl, 1999gh and 2000B) that are out of the "main sequence" of the distribution. These three BLs are on the lower side of $R_V = 2.0$ line and this result is consistent with previous studies that SNe Ia with high Si II $\lambda 6355$ expansion velocity have redder colors and prefer a lower R_V (e.g., Wang et al. 2009; Foley & Kasen 2011). Note that though relatively large EW(6100) labels SN 1999gh as BL, SN 1999gh also has a large EW(5750), which moves it up into the CL sub-type region in the Branch diagram (see figure 2 of Branch et al. 2009). SN 2000B has no EW measurements in Branch et al. (2009). CL objects have intrinsically red colors because of their low temperature. If SN 1999gh and 2000B are actually CL sub-type, then the distribution is attributed mostly to intrinsic color rather than interstellar dust.

Next we examine the color dependence on host morphology. In figure 2, different symbols show the different host morphological groups (circles; E/S0, pentagons; from Sa to Sb and stars; Sc or later and Irr). A trend can be seen that SNe Ia whose hosts are early-type spirals (pentagons) have the reddest color along with the dust extinction with $R_V = 2.0$. This result implies that there is intrinsic color offset depending on the host galaxy morphology as it has been said in previous studies (e.g., Sullivan et al. 2010; Pan et al. 2014). The breakdown of the host morphological dependence is shown in figure 3. Although the sample size is not large, figure 3 shows the trend seen in figure 2, SNe Ia which occur in early-type spirals have the reddest color, holds even after divided into Branch sub-types.

The effect of $s_{(B)}$ on the $B - V$ and $V - R$ colors is inferred from equations (1), (2) and the R -band regression of the bluest SNe Ia². In figure 2, the blue arrow shows the variations of colors for the bluest SNe Ia when $s_{(B)}$ varies from $s_{(B)} = 0.8$ to $s_{(B)} = 1.2$. It is expected that colors for most objects will move towards the dust extinction lines. The two BL objects (SN 1999gh and 2000B) however, have small $s_{(B)}$ ($s_{(B)} = 0.756$ and 0.854 , respectively) and stretch effect cannot explain the peculiar red colors.

We also investigate the relation between $B - V$ color and Si II $\lambda 6355$ absorption line velocity. We use the Si II velocity measured within ± 7 days from maximum brightness phase obtained by Blondin et al. (2012) (see also table 1). In figure 4, SN 1999cl and 1999gh BL objects which show peculiar red $B - V$ and $V - R$ colors have typical values of Si II velocity (SN 2000B has no velocity measurements).

3.2 ΔM_B vs $SNCE$

In this section, we examine the ΔM_B and $SNCE$ parameters introduced by TAK17. ΔM_B is sensitive to distance to an object, so nearby SN Ia has a large uncertainty of ΔM_B since it will be affected by the peculiar velocity (σ_V) of its host galaxy. Therefore, we plot samples whose total magnitude uncertainty, $\sigma_{total} = \sqrt{\sigma_m^2 + \sigma_{phot.}^2}$ is less than 0.30 mag. σ_m is a magnitude uncertainty caused by the peculiar velocity $\sigma_m = \frac{5 \sigma_V}{cz \ln(10)}$, where c is the speed of light and z is the redshift. $\sigma_{phot.}$ is an uncertainty from photometry. Here we adopt a typical peculiar velocity in the local Universe $\sigma_V = 300$ km/s and 23 SNe Ia in the Branch sample passed the criterion (hereafter referred to as "Branch sub-sample"). We plot the Branch sub-sample on the ΔM_B and $SNCE$ diagram in figure 5.

In TAK17, they showed statistically that the sample whose host color is blue (red) has a small (large) value of $SNCE$ and the both samples may obey multiple dust extinction laws. Using SNe Ia with typical stretch factor ($0.9 < s_{(B)} < 1.1$), they obtained extinction law with $R_V = 2.0^{+0.2}_{-0.1}$ from the sample whose host color is red ($u - r > 2.5$) and that with $R_V = 3.7^{+0.3}_{-0.4}$ from the sample whose host color is blue ($u - r < 2.0$). In figure 5, we show different dust extinction laws. Black solid line denotes dust extinction similar to that of our Milky-Way ($R_V = 3.1$) and red dashed line shows an extinction law with small $R_V = 2.0$. Most of our samples become to be consistent with the Milky-Way like extinction law after stretch correction. On the other hand, there are some outliers whose $SNCE$ are large (SN 1999cl, 1999gh and 2000B) compared to the other objects with similar ΔM_B .

In figure 6, we plot the ΔM_B and $SNCE$ diagram colored by the host morphology. The objects whose hosts are early-type spirals (Sa-Sb) are distributed along with the Milky-Way like

² $(M_B - M_V) = 0.12 \times s_{(B)}^{-1} - 0.22$ and $(M_V - M_R) = 0.34 \times s_{(B)}^{-1} - 0.36$

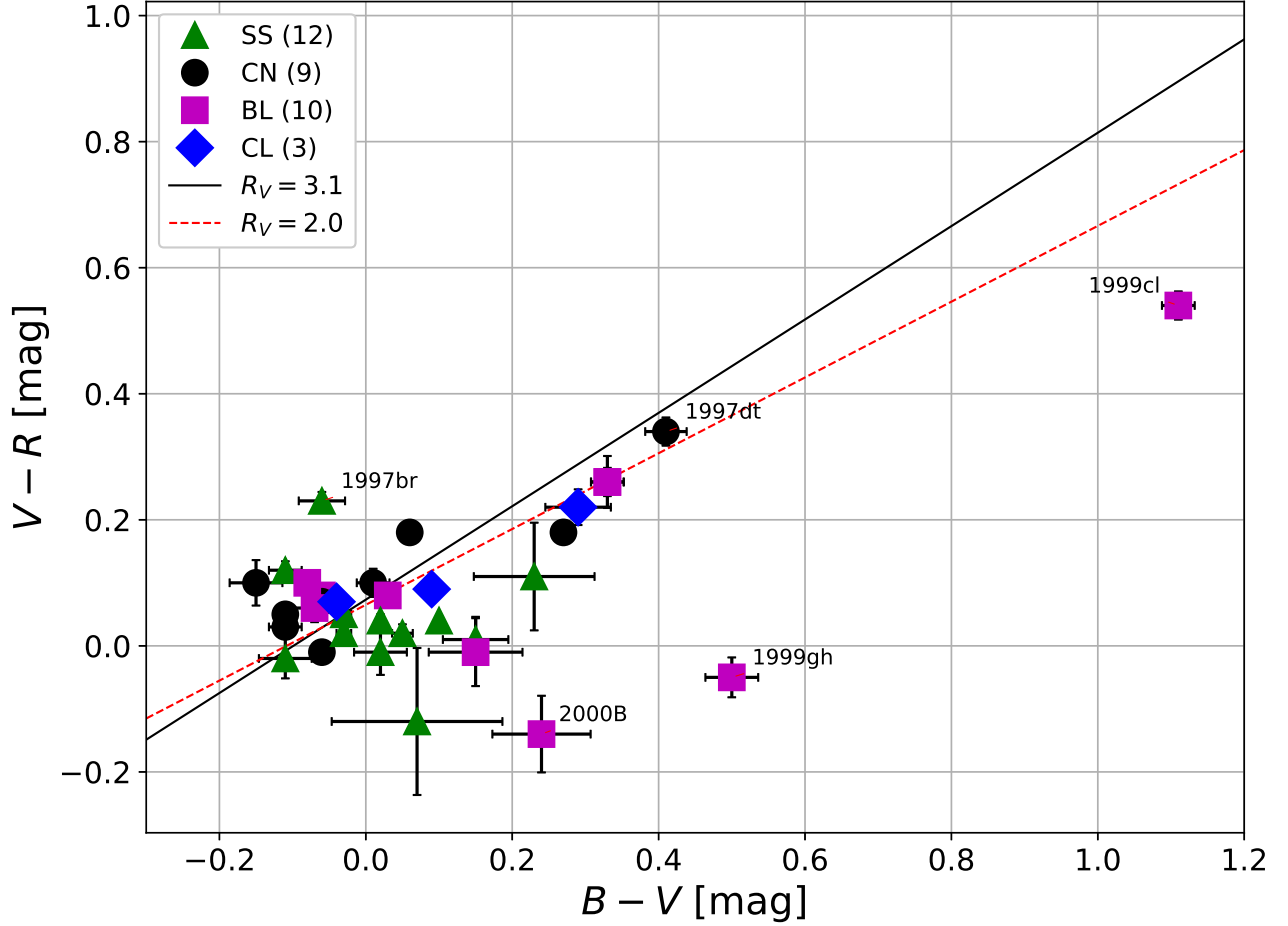


Fig. 1: $B - V$ vs $V - R$ color-color diagram. Different symbols show different Branch sub-types. Numbers in the brackets indicate the number of each Branch sub-type sample. Black solid and red dashed lines represent dust extinction laws with $R_V = 3.1$ (Milky-Way like) and $R_V = 2.0$ calculated using Cardelli et al. (1989), respectively. We draw these lines in order to pass across the main cluster around $B - V \sim V - R \sim 0$.

extinction line. Among the three BL outliers with peculiar red SNE colors, two objects (SN 1999gh and 2000B) are occurred in early-type (E/S0) galaxies. To increase sample size, we make a subset of 67 objects from TAK08 with $\sigma_{total} < 0.30$ mag (hereafter referred to as "TAK08 photometric sub-sample") which will be discussed in section 4.3. The list of the TAK08 photometric sub-sample is shown in table 3. We added TAK08 photometric sub-sample shown by white filled circles in figure 6 and 7.

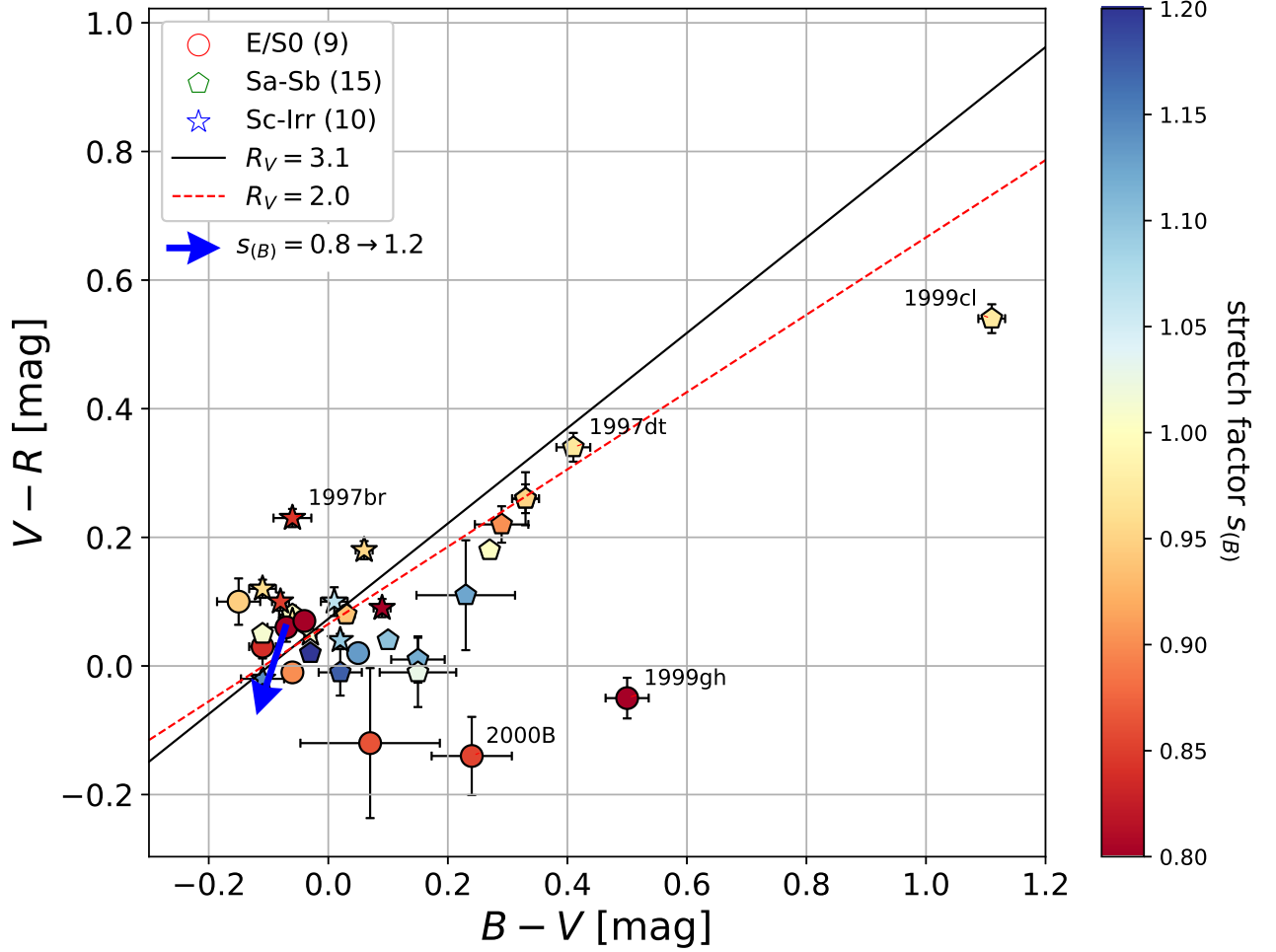


Fig. 2: $B - V$ vs $V - R$ color-color diagram with host galaxy morphology and $s_{(B)}$. Circles, pentagons and stars indicate objects whose hosts are elliptical or lenticular galaxies (E/S0; $T \leq 0$), early-type spirals (from Sa to Sb; $1 \leq T \leq 4$), and late-type spirals or irregular galaxies (Sc or later and Irr; $T \geq 5$), respectively. The color bar indicates the B -band stretch factor $s_{(B)}$ of SNe Ia. For reference, the blue arrow shows the variation of the bluest SNe Ia colors when $s_{(B)}$ varies from 0.8 to 1.2. The lines presented here are the same as in figure 1.

3.3 The distribution of $SNCE$

In TAK17, they suggest that there may be different populations on the $\Delta M_B - SNCE$ diagram. That means there may be sub-types with intrinsically different color and dust extinctions. We examined the distribution of $SNCE$ difference between CN and BL sub-types, both of which have typical values of stretch factor $s_{(B)}$. We apply Kolmogorov–Smirnov (KS) test to check if their probability distributions are different or not. As a result, we found the p-value is 0.41 and there is no difference in their distributions at the 5% significant level. However, our sample is not enough in numbers, so it is

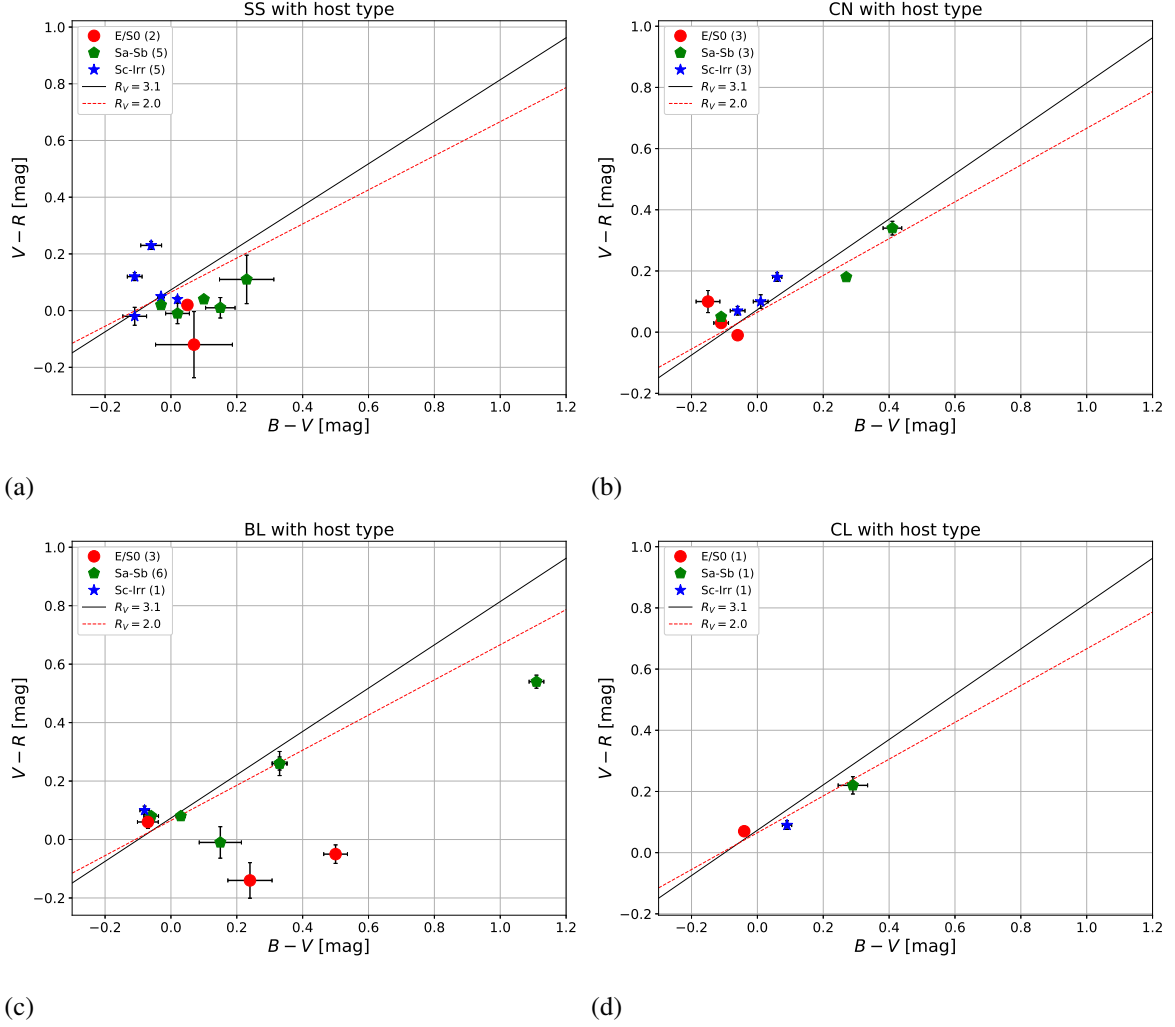


Fig. 3: $B - V$ vs $V - R$ diagrams with host galaxy morphology. Each figure shows the Branch sample of (a) Shallow Silicon, (b) Core Normal, (c) Broad Line and (d) Cool objects, respectively. The red and black lines presented here are the same as in figure 1.

desired to obtain the larger number of sample with Branch sub-type classification to test the validity.

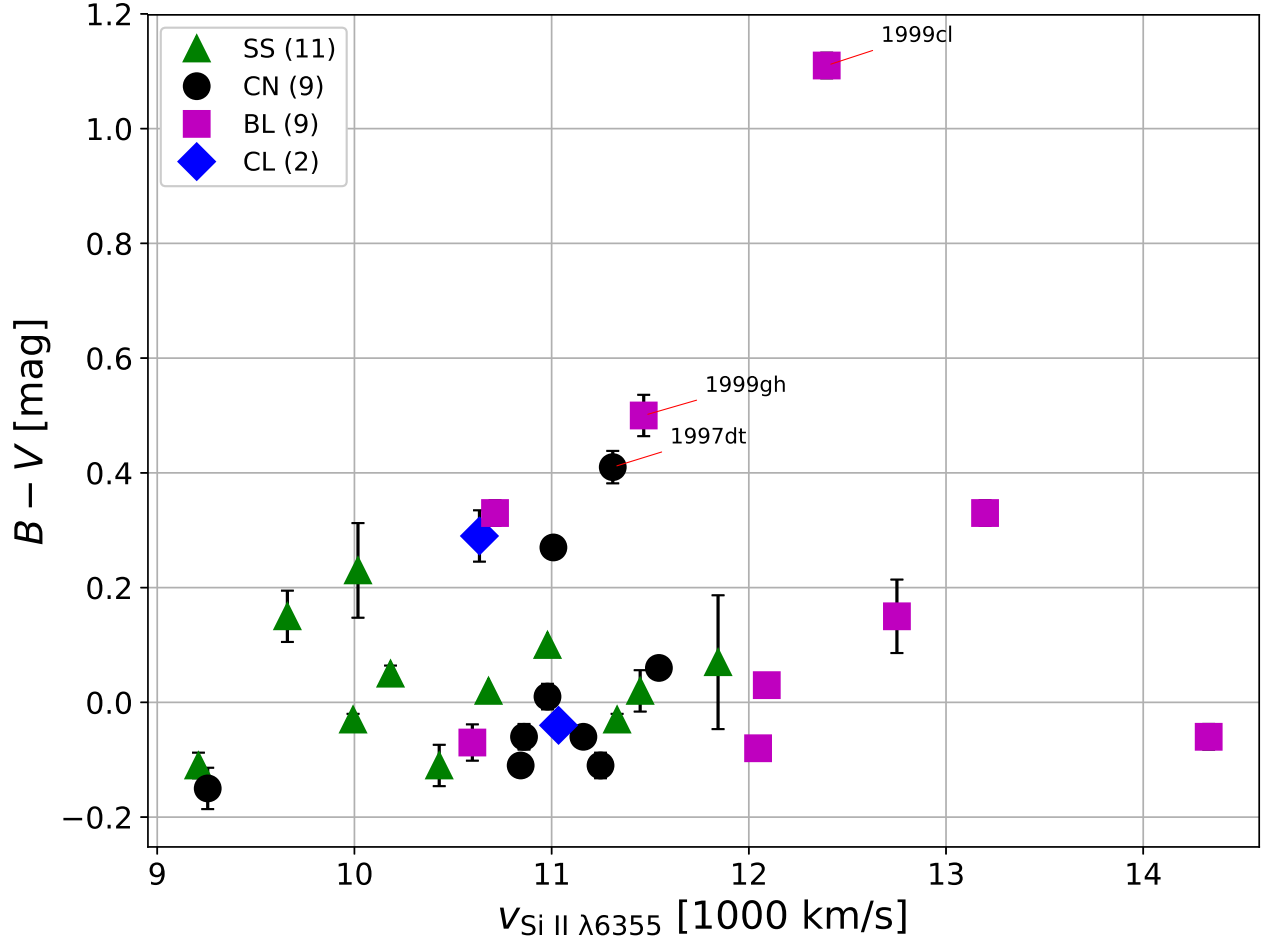


Fig. 4: The relation of the Si II $\lambda 6355$ absorption line velocity (hereafter v_{6355}) and $B - V$ color. The value of v_{6355} is derived from Blondin et al. (2012). SN 1997br, 2000B and 2000cn have no velocity measurements.

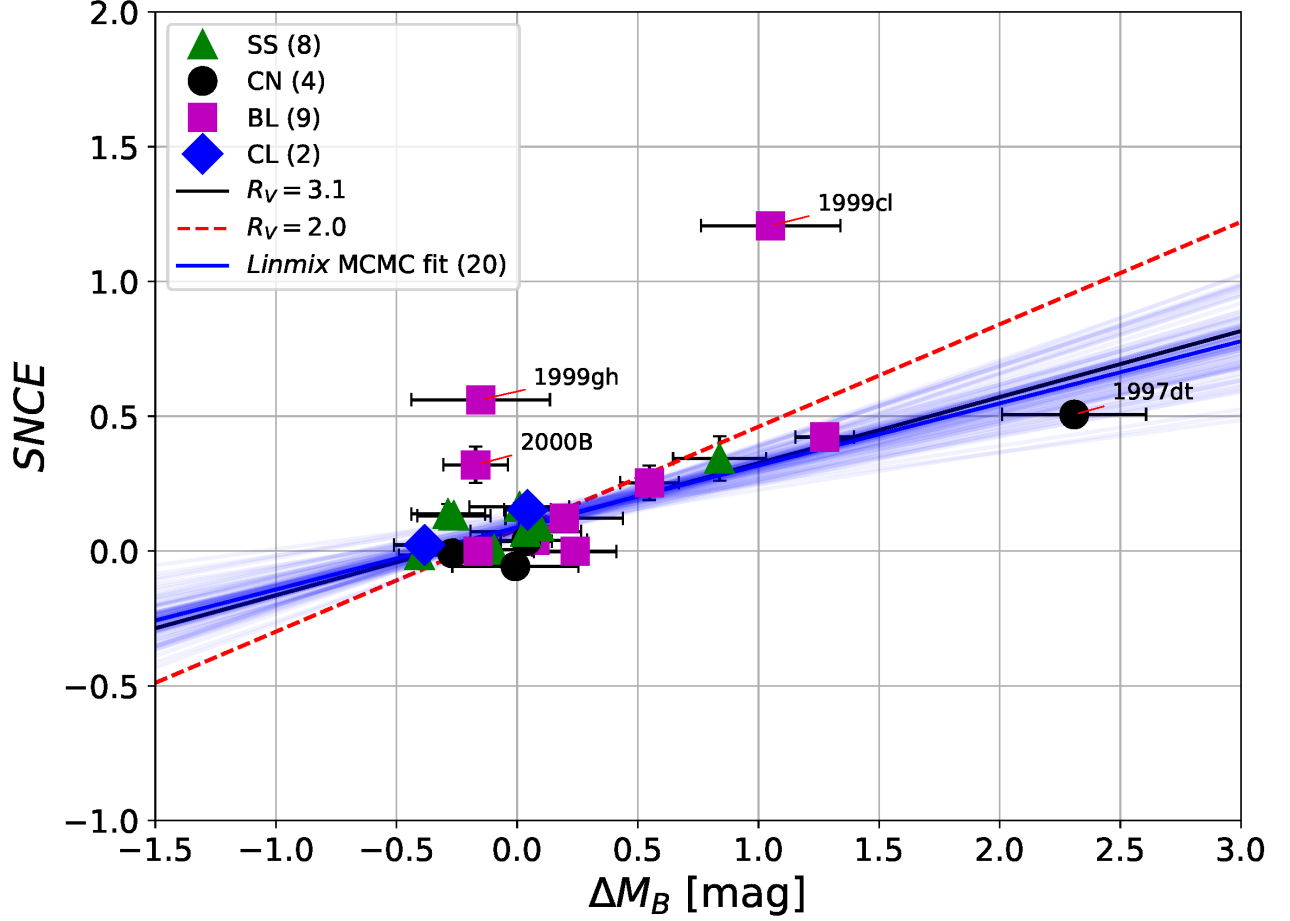


Fig. 5: The $\Delta M_B - SNCE$ diagram of the Branch sub-sample. Black solid and red dashed lines denote different dust extinctions with $R_V = 3.1$ and $R_V = 2.0$ respectively. The solid blue line shows the average of linmix MCMC fit results to the 20 samples excluding three BL outliers (SN 1999cl, 1999gh, and 2000B), with 100 random MCMC fit lines overlaid as light blue.

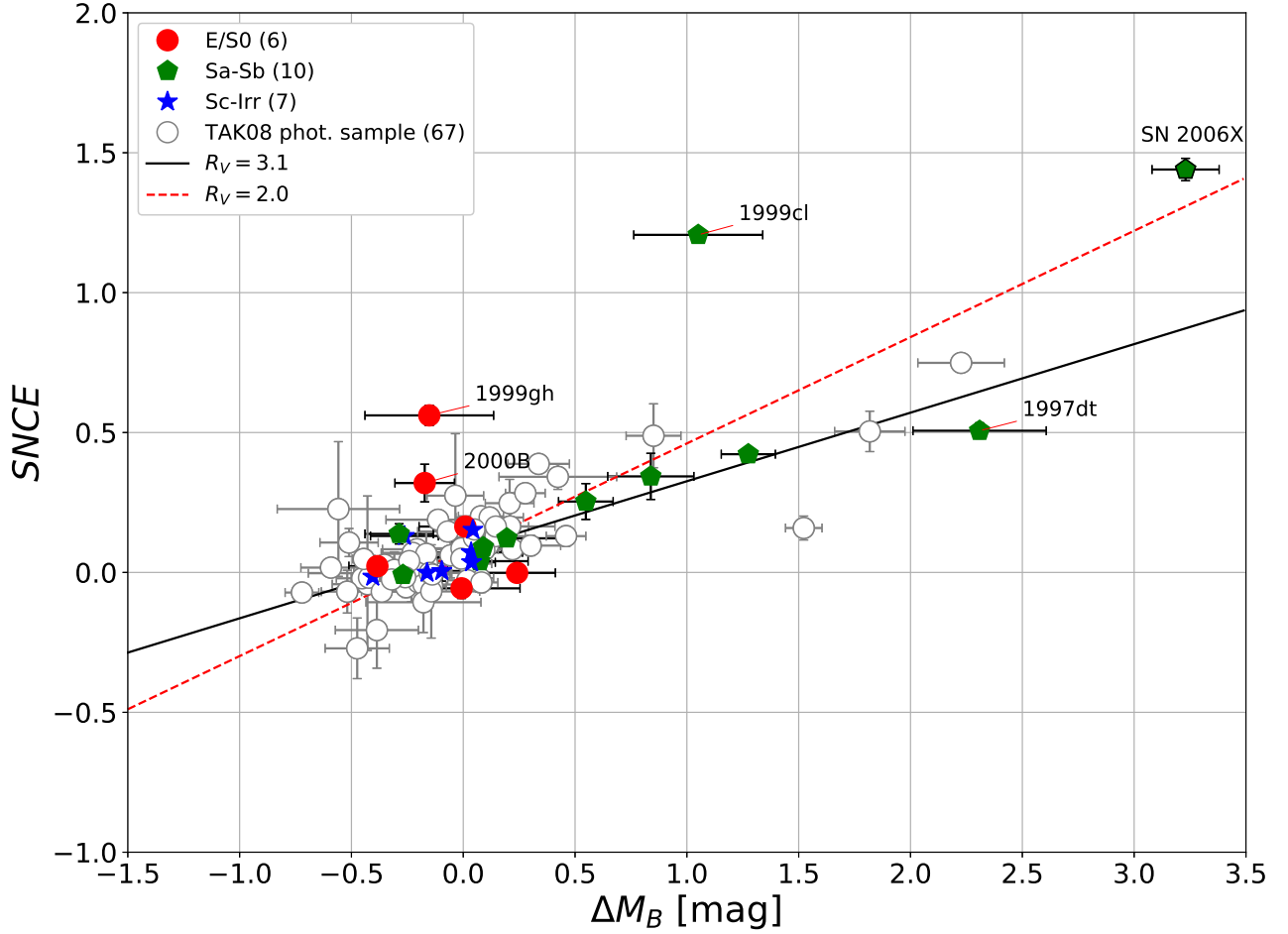


Fig. 6: The $\Delta M_B - SNCE$ diagram colored by the host galaxy morphology. TAK08 photometric sub-sample is shown by white filled circles. We also include SN 2006X, a BL sub-type SN Ia with high-extinction for comparison (see section 4.2).

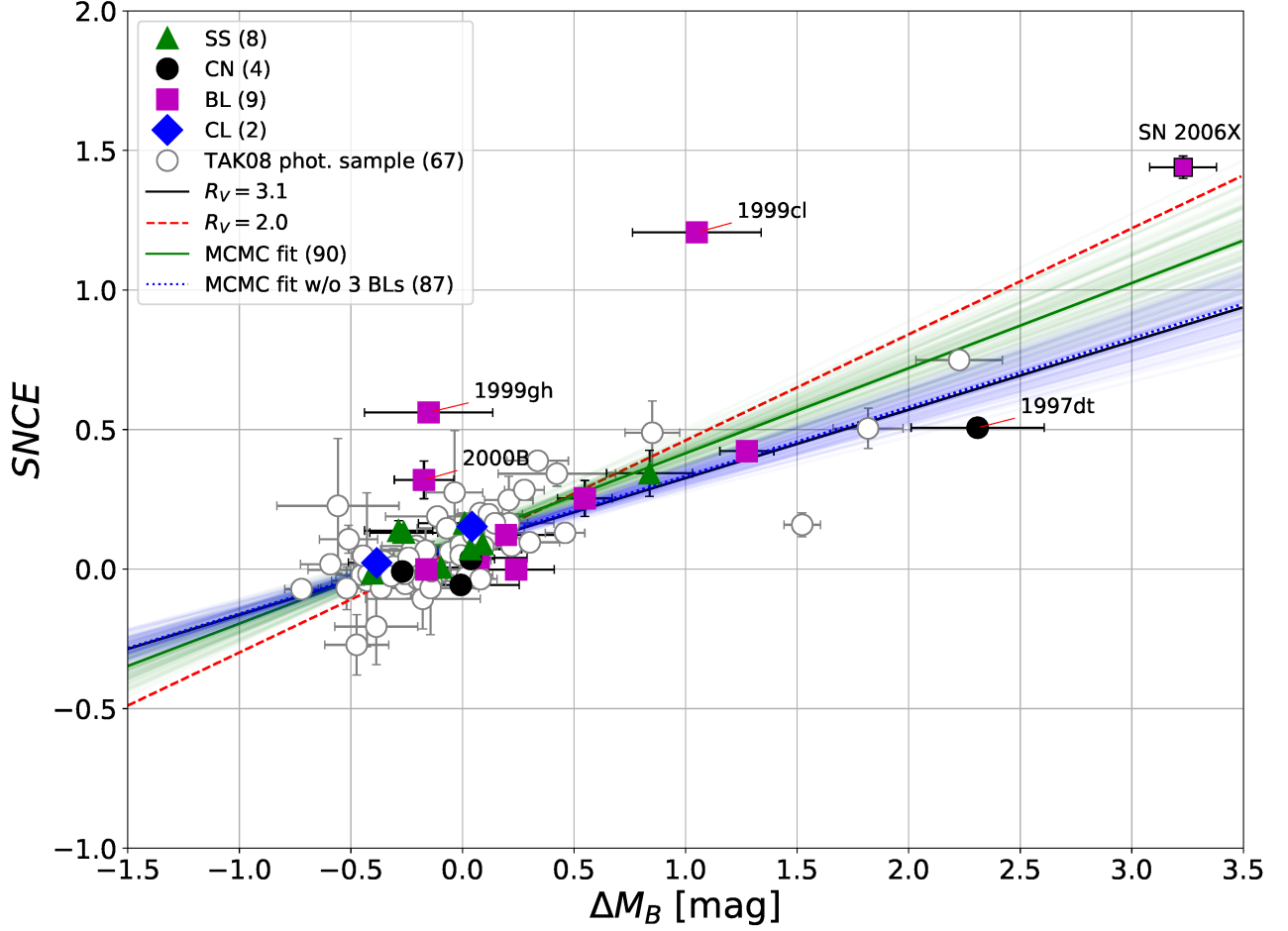


Fig. 7: The $\Delta M_B - SNCE$ diagram including the TAK08 photometric sub-sample marked as white filled circles. The green lines show the result of MCMC fit to all Branch sub-sample + TAK08 photometric sub-sample while the blue lines show the result without the three BL outliers. For more detailed descriptions of other lines, see the caption in figure 5. We also include SN 2006X, a BL sub-type SN Ia with high-extinction for comparison (see section 4.2).

Table 1: Photometric and spectroscopic information of the Branch sample and the host galaxies

SN name	Branch* sub-type	$s_{(B)}^{\dagger}$	B^{\ddagger}	V^{\S}	R^{\parallel}	EW(6100) [#] (Å)	EW(5750) ^{**} (Å)	$v_{6355}^{\dagger\dagger}$ (km/s)	Phase ^{††} of spectrum (day)	Wang ^{§§} class	Host name	$cz^{\#\#}$ (km/s)	Host ^{***} morphology	Host T index
1989B	CL	0.902(0.021)	-18.69(0.04)	-18.98(0.02)	-19.20(0.02)	126	25	-10634	-1.3	N	NGC 3627	727	SAB(s)b	3
1991T	SS	1.119(0.025)	-20.77(0.04)	-20.92(0.02)	-20.93(0.03)	27	3	-9660	-1.5	91T	NGC 4527	1736	SAB(s)bc	4
1994D	CN	0.838(0.010)	-18.49(0.02)	-18.38(0.01)	-18.41(0.01)	98	21	-11248	-0.1	N	NGC 4526	617	SAB(s)0 ⁺ 0	-2
1994ae	CN	1.067(0.015)	-18.68(0.01)	-18.69(0.02)	-18.79(0.01)	87	10	-10979	0.0	N	NGC 3370	1279	SA(s)c	5
1996X	CN	0.900(0.006)	-19.63(0.01)	-19.57(0.01)	-19.56(0.01)	85	20	-11161	0.1	N	NGC 5061	2082	E0	-5
1997br	SS	0.845(0.016)	-19.37(0.03)	-19.31(0.01)	-19.54(0.01)	-	-	-	-	-	ESO 576-40	2085	Sd/Irr	7
1997do	BL	1.002(0.011)	-18.95(0.02)	-18.89(0.01)	-18.97(0.01)	-	-	-14332	-6.6	HV	UGC 3845	3034	Sbc	4
1997dt	CN	0.971(0.009)	-16.66(0.02)	-17.07(0.02)	-17.41(0.01)	87	14	-11310	0.2	N	NGC 7448	2194	Sbc	4
1998V	CN	1.012(0.007)	-19.31(0.01)	-19.20(0.00)	-19.25(0.01)	84	19	-10843	0.3	N	NGC 6627	5268	Sb	3
1998ab	SS	0.958(0.011)	-19.35(0.02)	-19.24(0.01)	-19.36(0.01)	-	-	-9209	6.7	91T	NGC 4704	8134	Sc	5
1998bu	CN	1.003(0.005)	-19.09(0.01)	-19.36(0.00)	-19.54(0.01)	93	21	-11009	-1.6	N	NGC 3368	897	Sab	2
1998dh	BL	0.937(0.005)	-18.71(0.01)	-18.74(0.01)	-18.82(0.01)	120	24	-12091	-0.6	N	NGC 7541	2678	Sbc	4
1998ec	BL	1.029(0.023)	-18.52(0.04)	-18.67(0.05)	-18.66(0.02)	124	11	-12751	-3.0	HV	UGC 3576	5966	Sb	3
1998eg	CN	0.970(0.031)	-18.93(0.02)	-18.87(0.01)	-18.94(0.01)	95	20	-10860	-0.8	N	UGC 12133	7423	Sc	5
1998es	SS	1.132(0.016)	-19.21(0.01)	-19.26(0.01)	-19.28(0.01)	51	7	-10183	-0.5	91T	NGC 632	3168	S0	0
1999aa	SS	1.143(0.026)	-19.33(0.02)	-19.22(0.03)	-19.20(0.01)	63	14	-10430	-0.2	91T	NGC 2595	4330	Sc	5
1999ac	SS	1.015(0.010)	-19.01(0.01)	-18.98(0.00)	-19.03(0.00)	84	9	-9993	0.4	91T	NGC 6063	2848	Scd	6
1999cc	BL	0.850(0.012)	-18.88(0.01)	-18.80(0.01)	-18.90(0.01)	121	26	-12047	-0.2	N	NGC 6038	9392	Sc	5
1999cl	BL	0.972(0.019)	-17.92(0.02)	-19.03(0.01)	-19.57(0.02)	133	19	-12395	0.7	HV	NGC 4501	2281	Sb	3
1999dq	SS	1.094(0.004)	-19.43(0.00)	-19.45(0.00)	-19.49(0.01)	51	10	-10680	0.4	91T	NGC 976	4295	Sc	5
1999ee	SS	1.124(0.016)	-18.37(0.02)	-18.60(0.08)	-18.71(0.03)	77	9	-10018	-0.2	N	IC 5179	3422	SA(rs)bc	4
1999ej	BL	0.792(0.021)	-18.33(0.03)	-18.26(0.01)	-18.32(0.02)	108	27	-10598	1.1	N	NGC 495	4114	S0/Sa	0
1999gd	BL	0.942(0.010)	-17.64(0.02)	-17.97(0.01)	-18.23(0.02)	108	17	-10713	1.1	N	NGC 2623	5535	Sa	1
1999gh	BL	0.756(0.016)	-18.62(0.02)	-19.12(0.03)	-19.07(0.01)	-	-	-11467	5.5	N	NGC 2986	2302	E	-5
1999gp	SS	1.204(0.008)	-19.22(0.01)	-19.19(0.00)	-19.21(0.01)	52	8	-11332	0.0	91T	UGC 1993	8018	Sb	3
2000B	BL	0.854(0.029)	-18.90(0.03)	-19.14(0.06)	-19.00(0.01)	-	-	-	-	-	NGC 2320	5901	E	-5
2000E	SS	1.101(0.003)	-18.52(0.00)	-18.62(0.00)	-18.66(0.00)	78	13	-10979	-2.3	N	NGC 6951	1424	SAB(rs)bc	4
2000cn	CL	0.761(0.009)	-18.44(0.01)	-18.53(0.01)	-18.62(0.01)	-	-	-	-	-	UGC 11064	7043	Scd	6
2000cx	SS	0.863(0.055)	-19.34(0.06)	-19.41(0.10)	-19.29(0.06)	49	3	-11844	-0.3	*	NGC 524	2379	S0	0
2000dk	CL	0.762(0.008)	-18.87(0.01)	-18.83(0.01)	-18.90(0.01)	124	47	-11035	0.8	N	NGC 382	5228	E	-5
2001V	SS	1.174(0.021)	-19.56(0.02)	-19.58(0.03)	-19.57(0.02)	-	-	-11449	-3.3	91T	NGC 3987	4361	Sb	3
2001el	CN	0.953(0.012)	-18.14(0.01)	-18.20(0.01)	-18.38(0.01)	95	14	-11544	1.2	N	NGC 1448	1164	SAd	6
2002bo	BL	0.951(0.024)	-17.92(0.02)	-18.25(0.01)	-18.51(0.04)	147	13	-13198	-0.6	HV	NGC 3190	1271	SA(s)a pec	1
2004S	CN	0.946(0.016)	-18.93(0.02)	-18.78(0.03)	-18.88(0.02)	89	13	-9256	1.6	N	MCG -05-16-21	2516	S	-2
2006X ^{†††}	BL	0.858(0.025)	-15.51(0.14)	-16.87(0.14)	-17.41(0.14)	179	9	-15680	1.3	HV	NGC 4321	1557	Sbc	4

* Branch et al. (2009). [†], [‡], [§], ^{||} Takanashi et al. (2008). The 1σ error is given in between parenthesis. [#], ^{**} Branch et al. (2009). ^{††}, ^{‡‡}, ^{§§} Blondin et al. (2012). ^{††} It is the phase of v_{6355} measurement relative to B -band maximum.

^{|||} Branch et al. (2009) and Transient Name Server <<https://wis-tns.weizmann.ac.il/>> ^{##}, ^{***} NASA/IPAC Extragalactic Database <<https://ned.ipac.caltech.edu/>> We obtain cz of SN 2001el, 2001V and 2004S from individual publications (Krisciunas et al. 2003; van Driel et al. 2001; Misra et al. 2005, respectively). ^{†††} We add the SN 2006X in the list for comparison (see section 4.2). We convert the $\Delta m_{15}(B)$ parameter ($\Delta m_{15}(B) = 1.31 \pm 0.05$ mag from Wang et al. 2008) into $s_{(B)}$ by using the formula $s_{(B)} = (3.06 - \Delta m_{15}(B))/2.04$ of Jha et al. (2006). We calculate the B, V, R -band absolute magnitudes using the apparent magnitudes at maximum (Wang et al. 2008) and the Cepheid distance modulus ($\mu = 30.91 \pm 0.14$ mag; Freedman et al. 2001).

Table 2: ΔM_B and $SNCE$ of the Branch sample

SN name	Branch sub-type	ΔM_B^*	$SNCE^\dagger$
1989B	CL	0.14(0.90)	0.38(0.04)
1991T	SS	-1.57(0.38)	0.26(0.04)
1994D	CN	0.20(1.06)	-0.03(0.02)
1994ae	CN	0.45(0.51)	0.12(0.02)
1996X	CN	-0.80(0.31)	0.03(0.01)
1997br	SS	-0.66(0.32)	0.02(0.03)
1997do	BL	0.07(0.22)	0.04(0.02)
1997dt	CN	2.31(0.30)	0.51(0.03)
1998V	CN	-0.27(0.12)	-0.01(0.01)
1998ab	SS	-0.40(0.09)	-0.02(0.02)
1998bu	CN	-0.06(0.73)	0.37(0.01)
1998dh	BL	0.20(0.24)	0.12(0.01)
1998ec	BL	0.55(0.12)	0.25(0.06)
1998eg	CN	0.04(0.11)	0.04(0.02)
1998es	SS	0.01(0.21)	0.16(0.01)
1999aa	SS	-0.10(0.16)	0.01(0.04)
1999ac	SS	0.04(0.23)	0.07(0.01)
1999cc	BL	-0.16(0.08)	-0.00(0.01)
1999cl	BL	1.05(0.29)	1.21(0.02)
1999dq	SS	-0.26(0.15)	0.13(0.00)
1999ee	SS	0.84(0.19)	0.34(0.08)
1999ej	BL	0.24(0.17)	-0.00(0.03)
1999gd	BL	1.27(0.12)	0.42(0.02)
1999gh	BL	-0.15(0.29)	0.56(0.04)
1999gp	SS	0.09(0.08)	0.09(0.01)
2000B	BL	-0.17(0.13)	0.32(0.07)
2000E	SS	0.66(0.46)	0.21(0.00)
2000cn	CL	0.04(0.10)	0.15(0.01)
2000cx	SS	-0.59(0.31)	0.15(0.12)
2000dk	CL	-0.38(0.13)	0.02(0.01)
2001V	SS	-0.29(0.15)	0.14(0.04)
2001el	CN	0.80(0.56)	0.15(0.01)
2002bo	BL	1.01(0.51)	0.42(0.02)
2004S	CN	-0.01(0.24)	-0.06(0.04)
2006X [‡]	BL	3.23(0.15)	1.44(0.04)

^{*}, [†] The 1σ error is given in between parentheses.

[‡] We also include SN 2006X in the list for comparison (see section 4.2).

Table 3: TAK08 photometric sub-sample

SN name	cz (km/s)	ΔM_B	$SNC E$
1990O	9113	-0.22(0.09)	0.00(0.03)
1990T	11821	0.21(0.11)	0.25(0.09)
1990Y	10664	0.85(0.12)	0.49(0.11)
1990af	14837	-0.35(0.06)	0.03(0.01)
1991S	16213	-0.39(0.19)	-0.21(0.14)
1991U	9320	-0.23(0.10)	-0.02(0.08)
1991ag	4296	-0.21(0.15)	0.08(0.04)
1992J	13276	-0.04(0.13)	0.27(0.22)
1992K	3313	-0.56(0.27)	0.23(0.24)
1992P	7853	-0.14(0.09)	-0.01(0.02)
1992ae	21966	-0.16(0.08)	0.03(0.06)
1992al	4180	-0.43(0.16)	-0.04(0.01)
1992aq	29382	-0.26(0.09)	-0.05(0.04)
1992au	18186	-0.43(0.26)	-0.00(0.28)
1992bc	5959	-0.45(0.12)	-0.02(0.03)
1992bg	10381	-0.20(0.09)	-0.01(0.04)
1992bh	13276	0.22(0.06)	0.08(0.03)
1992bk	17021	-0.31(0.10)	0.01(0.06)
1992bl	12697	-0.42(0.08)	-0.02(0.04)
1992bo	5517	-0.22(0.12)	0.01(0.03)
1992bp	23047	-0.72(0.08)	-0.07(0.02)
1992br	25696	-0.52(0.12)	-0.07(0.08)
1992bs	18510	0.07(0.06)	-0.02(0.05)
1993B	20211	-0.14(0.06)	-0.05(0.03)
1993H	7208	0.08(0.10)	0.20(0.03)
1993O	15305	-0.20(0.06)	-0.04(0.03)
1993ac	14511	-0.06(0.08)	0.06(0.08)
1993ae	5669	-0.51(0.13)	0.11(0.05)
1993ag	14772	0.11(0.09)	0.10(0.03)
1993ah	8712	-0.47(0.14)	-0.27(0.11)
1994M	6889	0.02(0.10)	0.03(0.03)
1994Q	8595	0.07(0.13)	0.12(0.10)
1994S	4792	-0.23(0.14)	0.07(0.03)
1995D	2277	-0.20(0.29)	-0.00(0.02)
1995E	3499	2.23(0.19)	0.75(0.03)
1995ac	14772	-0.45(0.05)	0.05(0.01)
1995ak	6765	-0.17(0.19)	0.07(0.08)
1995bd	4770	0.34(0.14)	0.39(0.01)
1996C	8033	0.46(0.09)	0.13(0.04)
1996Z	2577	0.42(0.26)	0.34(0.04)
1996ab	17633	1.52(0.08)	0.16(0.04)
1996bl	10664	-0.24(0.07)	0.04(0.03)
1996bv	4970	0.14(0.13)	0.13(0.02)
1997E	3994	-0.01(0.16)	0.09(0.01)

Table 3: (Continued)

SN name	cz (km/s)	ΔM_B	$SNC E$
1997Y	4947	-0.18(0.14)	-0.04(0.02)
1997bp	2811	-0.11(0.23)	0.19(0.01)
1997bq	2875	-0.18(0.26)	-0.11(0.11)
1997cw	5272	0.30(0.13)	0.10(0.04)
1997dg	10060	0.02(0.09)	-0.03(0.02)
1998dk	3597	0.21(0.20)	0.16(0.08)
1998dx	14772	-0.36(0.09)	-0.07(0.04)
1998ef	4992	-0.59(0.13)	0.02(0.02)
1999X	7439	-0.14(0.22)	-0.07(0.17)
1999cp	3079	-0.15(0.21)	-0.00(0.01)
1999dk	4161	0.09(0.16)	0.08(0.01)
1999ef	11153	0.08(0.07)	-0.04(0.04)
1999ek	5248	0.05(0.13)	0.12(0.01)
2000bh	6796	-0.01(0.10)	0.05(0.03)
2000bk	7541	0.28(0.09)	0.28(0.01)
2000ca	7015	-0.26(0.09)	-0.02(0.01)
2000ce	4858	1.82(0.16)	0.50(0.07)
2000cf	10664	-0.14(0.08)	-0.01(0.03)
2001ba	9154	-0.32(0.07)	-0.03(0.01)
2001bt	4355	0.12(0.15)	0.20(0.01)
2001cn	4621	0.05(0.14)	0.15(0.01)
2001cz	4902	-0.07(0.13)	0.15(0.01)
2001en	4476	0.15(0.15)	0.16(0.01)

4 Discussions

4.1 Color-color diagram

First, we discuss the $B - V$, $V - R$ color-color diagram. In figure 2, the distributions with host morphology show that SNe Ia that occur in early-type spirals, rather than late-type spirals, tend to have redder colors along with the dust extinction lines. The distribution trend mentioned above holds when divided into Branch sub-types (see figure 3). In figure 1 of Childress et al. (2013), using 115 SNe Ia from the Nearby Supernova Factory, they compared SNe Ia color, host galaxy stellar mass, specific star formation rate (sSFR) and metallicity. They found that SNe Ia with red color belong to galaxies with intermediate stellar mass and sSFR. Our findings are consistent with their result. In the Branch CN sample, there is no outlier object which deviates from the extinction lines. On the other hand, there are three outliers in BL sample (SN 1999cl, 1999gh and 2000B) and the two of them (SN 1999gh and 2000B) occur in elliptical galaxies. This implies that we can roughly distinguish CN and peculiar red BL SNe Ia with a color-color diagram. Mandel et al. (2014) reported that BL high-velocity (=HV) SNe Ia show intrinsic redder $B - V$ color (by ~ 0.06 mag) than normal-velocity events. In addition, smaller R_V are predominantly derived from HV SNe Ia (Wang et al. 2009) and some of our BLs in figure 1 are consistent with their results.

4.2 Outliers on the color-color and $\Delta M_B - SNCE$ diagrams

We discuss some outliers on the color-color and $\Delta M_B - SNCE$ diagrams. First we focus on the BL sub-type outliers: SN 1999cl, 1999gh and 2000B. The Si II $\lambda 6355$ velocity of SN 1999gh is $v_{6355} = -11,467$ km/s, which is relatively small among BL sub-type (SN 2000B has no measurements). The boundary between NV and HV SNe Ia is located at $\sim -12,200$ km/s (see figure 8 of Blondin et al. 2012). There is a large overlap between the CN and the NV SNe Ia, as well as between the BL and HV SNe Ia. So the Si II velocity may not be a major quantity to discriminate peculiar BL objects. SN 1999gh and 2000B have red color in $B - V$ but bluer in $V - R$ than SS objects. The host morphological types of the SN 1999gh and 2000B are both elliptical galaxies ($T = 5$), so they are in generally less-dusty environment. Therefore, it can be inferred that SN 1999gh and 2000B have intrinsic red $B - V$ colors considering their blue $V - R$ colors. Mandel et al. (2014) shows similar result that intrinsic color distributions of HV and normal SNe Ia exhibit significant discrepancies in $B - V$ and $B - R$ colors.

SN 1999cl has distinct red color ($B - V = 1.11$, $V - R = 0.54$) compared with the other BL objects. Its host galaxy type is Sb ($T = 3$), which often shows strong extinction. From the image of its discovery, SN 1999cl is located in the disk component of its host. The Si II $\lambda 6355$ velocity

of SN 1999cl is $v_{6355} = -12,395$ km/s, which is typical among BL sub-type, but the overall shape of its spectrum is much redder than others. Based on these facts, SN 1999cl can be suffered from significant host extinction. In Krisciunas et al. (2006), they obtained the value of $R_V = 1.55$ for SN 1999cl, which may imply the size of dust is very small ($\sim 10^{-3}\mu m$). But when we compare SN 1999cl with SN 1999gh and 2000B on the $\Delta M_B - SNCE$ diagram, another possibility is that SN 1999cl has intrinsically red color, and also is strongly reddened by Milky-Way type dust extinction. Given the distribution trend of sample with Sa-Sb host galaxies seen in figure 6, the latter is more likely.

We compared SN 1999cl with SN 2006X, another high-extinction SN Ia (Wang et al. 2008) and also is classified as BL (EW(6100), EW(5750) = 179, 9) in Branch et al. (2009). The host of SN 2006X (= NGC4321) is an Sbc-type galaxy, which is similar to that of SN 1999cl. In Blondin et al. (2009), they report that the variability in Na I D lines was found both in the spectra of SN 1999cl and 2006X. The Na I D variability is interpreted to be associated with CSM in the SN Ia progenitor system (Patat et al. 2007). SN 2006X has $B - V = 1.35$ and $V - R = 0.56$ colors at B -band maximum (Wang et al. 2008). The $V - R$ color of SN 2006X is nearly the same as SN 1999cl but the $B - V$ color is ~ 0.2 mag redder than that of SN 1999cl. The ΔM_B and $SNCE$ of SN 2006X are $\Delta M_B = 3.23 \pm 0.15$ and $SNCE = 1.44 \pm 0.04^3$ (see figure 6 and 7). The slope between SN 1999cl and 2006X is close to the slope of $R_V = 3.1$ line on the $\Delta M_B - SNCE$ diagram, suggesting that both SN 1999cl and 2006X have intrinsically red color (possibly by CSM) and they are highly extinguished by interstellar dust.

While most SS objects show bluer color in both $B - V$ and $V - R$, SN 1997br has bluer color in $B - V$ but redder color in $V - R$ (the fourth reddest color in the Branch sample in figure 1). Its host galaxy type is Sd/Irr ($T = 7$) and the morphological index is the largest in our sample, suggesting that the SN 1997br is in dusty environment. However, if considering its bluer color in $B - V$, the peculiar color may be intrinsic. In Li et al. (1999), they reported that the light curve and time evolution of the spectra of SN 1997br are similar to those of over-luminous type of SN 1991T. However, their locations in color-color diagram are different.

SN 1997dt suffers highest extinction but has a typical value of stretch factor ($s_{(B)} = 0.971$) among CN sample. In addition, the spectral features of SN 1997dt look similar to the other CNs but the flux of the spectrum was reduced in shorter wavelengths. Its host galaxy type is an early-spiral Sbc ($T = 4$) which often shows strong extinction.

³ We used the Cepheid-based distance modulus of 30.91 ± 0.14 mag (Freedman et al. 2001) for calculating ΔM_B .

4.3 Implications for intrinsic color of SNe Ia

Since ΔM_B and $SNCE$ are residuals from the stretch-magnitude/color relations of the bluest SNe Ia, $\Delta M_B - SNCE$ diagram tells us the information of intrinsic luminosity/color and extinction by dust. It is clear that there are three BL objects (SN 1999cl, 1999gh and 2000B) which have large $SNCE$ in figure 5. This means they show red color after correcting for $s_{(B)}$. As shown in figure 2, these three BLs have small stretch factors in the Branch sample. When stretch correction is performed, their colors move in the lower-left direction in figure 2 (shown as the blue arrow). In addition, two-thirds of the BLs (SN 1999gh and 2000B) occur in early-type (E/S0) galaxies, suggesting that BL objects whose hosts are E/S0 galaxies need to apply different stretch correction. Another possibility is that the progenitor scenarios (explosion mechanisms) of such BL objects may differ from typical SNe Ia.

It is possible that small R_V can be derived because the R_V is averaged both for normal SNe Ia and intrinsically red SNe Ia. We employ the Bayesian linear regression method by Kelly (2007) with its python package *linmix*⁴. In figure 5, the solid blue line shows the average of *linmix* MCMC fit results to the Branch sub-sample excluding three BL outliers (SN 1999cl, 1999gh and 2000B) with 100 random MCMC fit lines overlaid as light blue. As a result, the average regression line which corresponds to $R_V = 3.3^{+0.8}_{-0.6}$ well matches the Milky-Way like extinction with $R_V = 3.1$.

To make the result more robust, we include the TAK08 photometric sub-sample for the regression analysis. In figure 7, the green solid line shows the average of 100 MCMC fit results using all Branch sub-sample and TAK08 photometric sub-sample while the blue line shows the same result without three BL outliers (SN 1999cl, 1999gh and 2000B). The slope of the green line corresponds to $R_V = 2.3 \pm 0.3$, while that of the blue line is $R_V = 3.0^{+0.4}_{-0.3}$ which is almost identical to $R_V = 3.1$. Therefore the three BL outliers make R_V small. When we exclude such outliers, the extinction law for SNe Ia becomes close to $R_V = 3.1$.

When we use SNe Ia for cosmological studies to measure distance, excluding peculiar BL objects may give more accurate results. This could be done just to use two optical colors (e.g., $B - V$ and $V - R$) around the time of maximum brightness. In addition, further environmental studies will give us clues about the difference in progenitor scenarios among Branch sub-types.

Using early phase color information, Stritzinger et al. (2018) found that there are two distinct early populations with different early color evolution in $B - V$ and all blue events are of the Branch SS sub-type, while all early red events except for the peculiar 2000cx-like SN 2012fr are of the Branch CN or CL sub-types. It is also important to study the early color evolution with Branch sub-types.

⁴ <https://github.com/jmeyers314/linmix>

5 Summary

In this study, with Branch spectroscopic classification as well as host galaxy morphology, we investigate the diversity of color and dust extinction of nearby 34 SNe Ia ($z \lesssim 0.04$). We summarize our findings as below.

- In the $B - V, V - R$ color-color diagram, different distribution among different host galaxy morphology can be seen: SNe Ia which occur in early-type spirals have the reddest color. The distribution trend holds when divided into the Branch spectroscopic sub-types.
- The three BLs (SN 1999cl, 1999gh and 2000B) have red colors in the $\Delta M_B - SNCE$ diagram. Two of them (SN 1999gh and 2000B) can be explained by their intrinsic red colors, and their hosts are elliptical galaxies which usually have little interstellar dusts. On the other hand, 1999cl which occur in Sb type host can be explained by both its intrinsic red color and strong extinction by interstellar dust.
- In our sample, it is inferred that lower value of R_V parameter is not necessary to explain the color diversity of SNe Ia. In other words, it suggests that the extinction law for most of SNe Ia might be explained by the typical extinction law in the Milky Way ($R_V = 3.1$).

Our results suggest the possibility of typical host galaxy extinction law for SNe Ia as seen in the Milky Way. It was suggested by TAK17 that there seems to be two (or more) different sub-groups with different intrinsic colors and/or dust extinction laws, but we infer this may be caused by some objects with peculiar intrinsic red color.

6 Acknowledgments

We thank the anonymous referee for reading the paper carefully and providing thoughtful comments, many of which have resulted in changes to improve the revised version of the manuscript. This work was supported by JSPS KAKENHI Grant numbers 18H05223 and 18H04342. N.A. gratefully appreciates the financial support of Hattori International Scholarship Foundation (HISF) for a grant that made it possible to complete this study.

References

- Betoule, M., Kessler, R., Guy, J., et al. 2014, *Astronomy & Astrophysics*, 568, A22
- Blondin, S., Prieto, J. L., Patat, F., et al. 2009, *The Astrophysical Journal*, 693, 207
- Blondin, S., Matheson, T., Kirshner, R. P., et al. 2012, *The Astronomical Journal*, 143, 126
- Branch, D., Dang, L. C., & Baron, E. 2009, *Publications of the Astronomical Society of the Pacific*, 121, 238

- Branch, D., Dang, L. C., Hall, N., et al. 2006, *Publications of the Astronomical Society of the Pacific*, 118, 560
- Brown, P. J., & Crumpler, N. R. 2020, *The Astrophysical Journal*, 890, 45
- Burns, C. R., Stritzinger, M., Phillips, M. M., et al. 2011, *The Astronomical Journal*, 141, 19
- . 2014, *The Astrophysical Journal*, 789, 32
- Cardelli, J. A., Clayton, G. C., & Mathis, J. S. 1989, *The Astrophysical Journal*, 345, 245
- Childress, M., Aldering, G., Antilogus, P., et al. 2013, *The Astrophysical Journal*, 770, 108
- Cikota, A., Deustua, S., & Marleau, F. 2016, *The Astrophysical Journal*, 819, 152
- Clayton, G. C., Wolff, M. J., Sofia, U. J., Gordon, K. D., & Misselt, K. A. 2003, *The Astrophysical Journal*, 588, 871
- Conley, A., Guy, J., Sullivan, M., et al. 2010, *The Astrophysical Journal Supplement Series*, 192, 1
- Contreras, C., Hamuy, M., Phillips, M. M., et al. 2010, *The Astronomical Journal*, 139, 519
- de Vaucouleurs, G. 1959, in *Astrophysik IV: Sternsysteme / Astrophysics IV: Stellar Systems* (Springer Berlin Heidelberg), 275–310
- Filippenko, A. V. 1997, *Annual Review of Astronomy and Astrophysics*, 35, 309
- Filippenko, A. V., Richmond, M. W., Matheson, T., et al. 1992, *The Astrophysical Journal*, 384, L15
- Folatelli, G., Phillips, M. M., Burns, C. R., et al. 2010, *The Astronomical Journal*, 139, 120
- Foley, R. J., & Kasen, D. 2011, *The Astrophysical Journal*, 729, 55
- Freedman, W. L., Madore, B. F., Gibson, B. K., et al. 2001, *The Astrophysical Journal*, 553, 47
- Gal-Yam, A. 2017, in *Handbook of Supernovae* (Springer International Publishing), 195–237
- Goldhaber, G., Groom, D. E., Kim, A., et al. 2001, *The Astrophysical Journal*, 558, 359
- Guy, J., Astier, P., Baumont, S., et al. 2007, *Astronomy & Astrophysics*, 466, 11
- Hamuy, M., Phillips, M. M., Suntzeff, N. B., et al. 1996, *The Astronomical Journal*, 112, 2398
- I. Iben, J., & Tutukov, A. V. 1984, *The Astrophysical Journal*, 284, 719
- Jha, S., Riess, A. G., & Kirshner, R. P. 2007, *The Astrophysical Journal*, 659, 122
- Jha, S., Kirshner, R. P., Challis, P., et al. 2006, *The Astronomical Journal*, 131, 527
- Kelly, B. C. 2007, *The Astrophysical Journal*, 665, 1489
- Kelly, P. L., Hicken, M., Burke, D. L., Mandel, K. S., & Kirshner, R. P. 2010, *The Astrophysical Journal*, 715, 743
- Kessler, R., Becker, A. C., Cinabro, D., et al. 2009, *The Astrophysical Journal Supplement Series*, 185, 32
- Krisciunas, K., Prieto, J. L., Garnavich, P. M., et al. 2006, *The Astronomical Journal*, 131, 1639
- Krisciunas, K., Suntzeff, N. B., Candia, P., et al. 2003, *The Astronomical Journal*, 125, 166
- Li, W. D., Qiu, Y. L., Qiao, Q. Y., et al. 1999, *The Astronomical Journal*, 117, 2709
- Livio, M., & Mazzali, P. 2018, *Physics Reports*, 736, 1
- Maeda, K., & Terada, Y. 2016, *International Journal of Modern Physics D*, 25, 1630024
- Mandel, K. S., Foley, R. J., & Kirshner, R. P. 2014, *The Astrophysical Journal*, 797, 75
- Mandel, K. S., Narayan, G., & Kirshner, R. P. 2011, *The Astrophysical Journal*, 731, 120
- Mandel, K. S., Scolnic, D. M., Shariff, H., Foley, R. J., & Kirshner, R. P. 2017, *The Astrophysical Journal*, 842, 93
- Mannucci, F. 2005, *Astronomical Society of the Pacific Conference Series*, Vol. 342, *Rates and Progenitors of Type Ia Supernovae*, ed. M. Turatto, S. Benetti, L. Zampieri, & W. Shea, 140
- Maoz, D., & Mannucci, F. 2012, *Publications of the Astronomical Society of Australia*, 29, 447
- Mazzali, P. A., Chugai, N., Turatto, M., et al. 1997, *Monthly Notices of the Royal Astronomical Society*, 284, 151

Misra, K., Kamble, A. P., Bhattacharya, D., & Sagar, R. 2005, *Monthly Notices of the Royal Astronomical Society*, 360, 662

Moreno-Raya, M. E., Mollá, M., López-Sánchez, Á. R., et al. 2016, *The Astrophysical Journal*, 818, L19

Nobili, S., & Goobar, A. 2008, *Astronomy & Astrophysics*, 487, 19

Nomoto, K. 1982, *The Astrophysical Journal*, 253, 798

Nugent, P., Phillips, M., Baron, E., Branch, D., & Hauschildt, P. 1995, *The Astrophysical Journal*, 455, doi:10.1086/309846

Pan, Y.-C., Foley, R. J., Jones, D. O., Filippenko, A. V., & Kuin, N. P. M. 2020, *Monthly Notices of the Royal Astronomical Society*, 491, 5897

Pan, Y.-C., Sullivan, M., Maguire, K., et al. 2014, *Monthly Notices of the Royal Astronomical Society*, 438, 1391

Patat, F., Chandra, P., Chevalier, R., et al. 2007, *Science*, 317, 924

Phillips, M. M. 1993, *The Astrophysical Journal*, 413, L105

Phillips, M. M., Lira, P., Suntzeff, N. B., et al. 1999, *The Astronomical Journal*, 118, 1766

Phillips, M. M., Wells, L. A., Suntzeff, N. B., et al. 1992, *The Astronomical Journal*, 103, 1632

Quimby, R., Hoflich, P., & Wheeler, J. C. 2007, *The Astrophysical Journal*, 666, 1083

Riess, A. G., Press, W. H., & Kirshner, R. P. 1996, *The Astrophysical Journal*, 473, 88

Sako, M., Bassett, B., Becker, A., et al. 2008, *AJ*, 135, 348

Sako, M., Bassett, B., Becker, A. C., et al. 2018, *Publications of the Astronomical Society of the Pacific*, 130, 064002

Saselli, M., Ishida, E. E. O., Hillebrandt, W., et al. 2016, *Monthly Notices of the Royal Astronomical Society*, 460, 373

Schlegel, D. J., Finkbeiner, D. P., & Davis, M. 1998, *The Astrophysical Journal*, 500, 525

Smith, M., Sullivan, M., Wiseman, P., et al. 2020, *Monthly Notices of the Royal Astronomical Society*, 494, 4426

Spergel, D. N., Bean, R., Dore, O., et al. 2007, *The Astrophysical Journal Supplement Series*, 170, 377

Stanishev, V., Goobar, A., Amanullah, R., et al. 2018, *Astronomy & Astrophysics*, 615, A45

Stritzinger, M. D., Shappee, B. J., Piro, A. L., et al. 2018, *The Astrophysical Journal*, 864, L35

Sullivan, M., Conley, A., Howell, D. A., et al. 2010, *Monthly Notices of the Royal Astronomical Society*, no

Sullivan, M., Guy, J., Conley, A., et al. 2011, *The Astrophysical Journal*, 737, 102

Takanashi, N., Doi, M., & Yasuda, N. 2008, *Monthly Notices of the Royal Astronomical Society*, 389, 1577

Takanashi, N., Doi, M., Yasuda, N., et al. 2017, *MNRAS*, 465, 1274

van Driel, W., Marcum, P., Gallagher, J. S., et al. 2001, *Astronomy & Astrophysics*, 378, 370

Wang, X., Li, W., Filippenko, A. V., et al. 2008, *The Astrophysical Journal*, 675, 626

Wang, X., Filippenko, A. V., Ganeshalingam, M., et al. 2009, *The Astrophysical Journal*, 699, L139

Webbink, R. F. 1984, *The Astrophysical Journal*, 277, 355

Whelan, J., & I. Iben, J. 1973, *The Astrophysical Journal*, 186, 1007

Zheng, W., Kelly, P. L., & Filippenko, A. V. 2018, *The Astrophysical Journal*, 858, 104